A starlike 3-dimensional counterexample to the hot spots conjecture*

Rami Atar† Krzysztof Burdzy‡

October 14, 2026

Abstract

We construct a bounded Lipschitz domain in $\mathbb{R}^3$ that is starlike about the origin and whose first positive Neumann eigenvalue is simple. A corresponding eigenfunction, after a choice of sign, has its unique global maximum at the origin. The construction uses domains with increasingly fine angular structure and convergence to a weighted eigenvalue problem whose first positive eigenfunction is radial.

1 Introduction

Our main result is the following.

Theorem 1. *There exists a bounded Lipschitz domain $\Omega \subset \mathbb{R}^3$, starlike about 0, whose first positive Neumann eigenvalue is simple. A corresponding real eigenfunction u has a continuous representative on $\overline{\Omega}$ and, after a choice of sign, satisfies*

$$u(0) > u(x) \qquad (x \in \overline{\Omega} \setminus \{0\}). \tag{1}$$

In particular,

$$u(0) > \max_{x \in \partial\Omega} u(x). \tag{2}$$

Rauch's hot spots conjecture [20] asserts that a first nonconstant Neumann eigenfunction attains its extrema only on the boundary. Burdzy and Werner [7] disproved this for a planar domain with two holes. Bass and Burdzy [3] constructed examples with both extrema strictly in the interior, and Burdzy [4] obtained such an example with only one hole. Further numerical examples were given by Kleefeld [16]. For an overview, see Burdzy [5].

Positive results for planar domains include those of Bañuelos and Burdzy [2], the symmetry results of Jerison and Nadirashvili [12] and Pascu [19], the lip-domain theorem of Atar and Burdzy [1], and the triangle theorem of Judge and Mondal [13], together with its erratum [14]. More recently, OpenAI [18] presented a proof for smooth simply connected planar domains. Taking that result as an input, Burdzy [6] derived the non-strict hot-spots property for nonsmooth boundary.

*This is a first draft. An extended version is expected soon.

†Viterbi Faculty of Electrical and Computer Engineering, Technion–Israel Institute of Technology, Haifa, Israel. E-mail: `rami@technion.ac.il`.

‡Department of Mathematics, University of Washington, Seattle, Washington, USA. E-mail: `burdzy@uw.edu`.

In higher dimensions, Kennedy and Rohleder [15] proved positive results for classes extending planar lip domains and symmetric domains. In contrast, de Dios Pont [9] constructed convex counterexamples in sufficiently high dimensions. De Dios Pont, Hsu and Taylor [10] determined the sharp maximal ratio between the interior and boundary maxima; their Remark 1.11 also discusses counterexamples homeomorphic to a ball in dimensions at least three. The present result shows that failure is possible in dimension three even under the stronger geometric requirement of starlikeness.

1.1 Notation

We write $|x|$ for the Euclidean norm of $x \in \mathbb{R}^3$,

$$B(x,r) = \{y \in \mathbb{R}^3 : |y-x| < r\}, \qquad B_r = B(0,r), \qquad S^2 = \{x \in \mathbb{R}^3 : |x| = 1\}.$$

The measure dS is ordinary surface measure on S^2, normalized by $\int_{S^2} dS = 4\pi$. For $U \subset S^2$, $|U|$ denotes its surface area. The symbols $\overline{D}$ and ∂D denote the closure and boundary of a set D.

A domain D is *starlike about* 0 if $x \in D$ implies $tx \in D$ for every $0 \le t \le 1$. It is *centrally symmetric* if $D = -D$. A Lipschitz domain is one whose boundary is locally the graph of a Lipschitz function in suitable orthogonal coordinates, with the domain on one side of the graph. Corners are allowed.

For an open set D, $H^1(D)$ is the space of square-integrable functions with square-integrable first weak derivatives. A Neumann eigenfunction with eigenvalue λ is a nonzero $u \in H^1(D)$ satisfying

$$\int_D \nabla u \cdot \nabla w \, dx = \lambda \int_D uw \, dx \qquad (w \in H^1(D)).$$

On a bounded connected Lipschitz domain we number the eigenvalues, with multiplicities, as

$$0 = \lambda_0(D) < \lambda_1(D) \le \lambda_2(D) \le \cdots .$$

Thus $\lambda_1(D)$ is the first nonconstant eigenvalue, also called the second Neumann eigenvalue. All functions and variational spaces in the proof are real unless Fourier series are being used.

For a function on B_R we write $v(r,\omega) = v(r\omega)$ in polar coordinates. The tangential gradient $\nabla_{S^2} v(r,\omega)$ always refers to differentiation in ω on the unit sphere. Matrix transposition is denoted by T. The constants denoted by C may change from one occurrence to the next; their parameter dependence is specified where needed. The construction uses a large radius R, fixed before the small spacing parameter δ tends to zero.

1.2 Outline and organization

The domain contains the unit ball and extends to radius R along an explicitly chosen set of directions. As the angular spacing δ tends to zero, its Neumann problem converges to a weighted variational problem on B_R. The first positive eigenfunction of that limiting problem is radial and strictly decreasing. Uniform convergence of the actual eigenfunctions transfers the strict difference between the value at the origin and the boundary values. Central symmetry and interior derivative estimates locate the unique maximum exactly at the origin.

Section 2 defines the domains. Section 3 describes the limiting variational problem and its angular coefficient. Section 4 states the six auxiliary lemmas. Using these lemmas, Section 5 proves Theorem 1. All six lemma proofs are collected in Section 6.

2 Construction of the domains

2.1 Parameters

For $R > 1$, the spherical annulus between radii 1 and R is

$$\mathcal{A}_{1,R} = \{x \in \mathbb{R}^3 : 1 < |x| < R\}.$$

The domain will contain only selected directions in this annulus.

Choose $R > 1$ and set

$$\alpha = R^{-5/2}, \qquad \theta = \frac{\alpha}{4\pi}, \qquad h = 1 - \sqrt{1-\theta}. \tag{3}$$

The number θ is the limiting fraction of the sphere that will be retained; $\alpha = 4\pi\theta$ is its limiting area. The identity $2h - h^2 = \theta$ explains the choice of h.

The spacing parameter is $\delta > 0$. The order of choices is: choose R large enough, *fix it*, and then let $\delta \downarrow 0$. Constants in extension and convergence estimates may depend on this fixed R and its associated θ.

2.2 A subset of the plane: horizontal and vertical strips

For $t \in \mathbb{R}$, define

$$\operatorname{dist}(t, \delta\mathbb{Z}) = \min_{n\in\mathbb{Z}} |t - \delta n|.$$

The planar set to be retained is

$$P_{\delta,h} = \Big\{ y = (y_1, y_2) \in \mathbb{R}^2 : \operatorname{dist}(y_1, \delta\mathbb{Z}) < h\delta/2 \text{ or } \operatorname{dist}(y_2, \delta\mathbb{Z}) < h\delta/2 \Big\}. \tag{4}$$

Thus it is the union of vertical strips centered at $y_1 = \delta n$ and horizontal strips centered at $y_2 = \delta n$, each of total width $h\delta$.

It is *periodic* in the precise sense that

$$y \in P_{\delta,h} \quad \Longleftrightarrow \quad y + \delta a \in P_{\delta,h} \qquad (a \in \mathbb{Z}^2).$$

A *period square* is any square $\delta a + [0,\delta]^2$ on which this repeated pattern is represented once.

For $a = (a_1, a_2) \in \mathbb{Z}^2$, define the closed square

$$H_a = \prod_{\nu=1}^{2} \big[a_\nu\delta + h\delta/2,\ (a_\nu + 1)\delta - h\delta/2\big]. \tag{5}$$

Then

$$\mathbb{R}^2 \setminus P_{\delta,h} = \bigcup_{a\in\mathbb{Z}^2} H_a.$$

Each H_a has side length $(1-h)\delta$. The retained area in a period square is

$$\delta^2 - (1-h)^2\delta^2 = (2h - h^2)\delta^2 = \theta\delta^2.$$

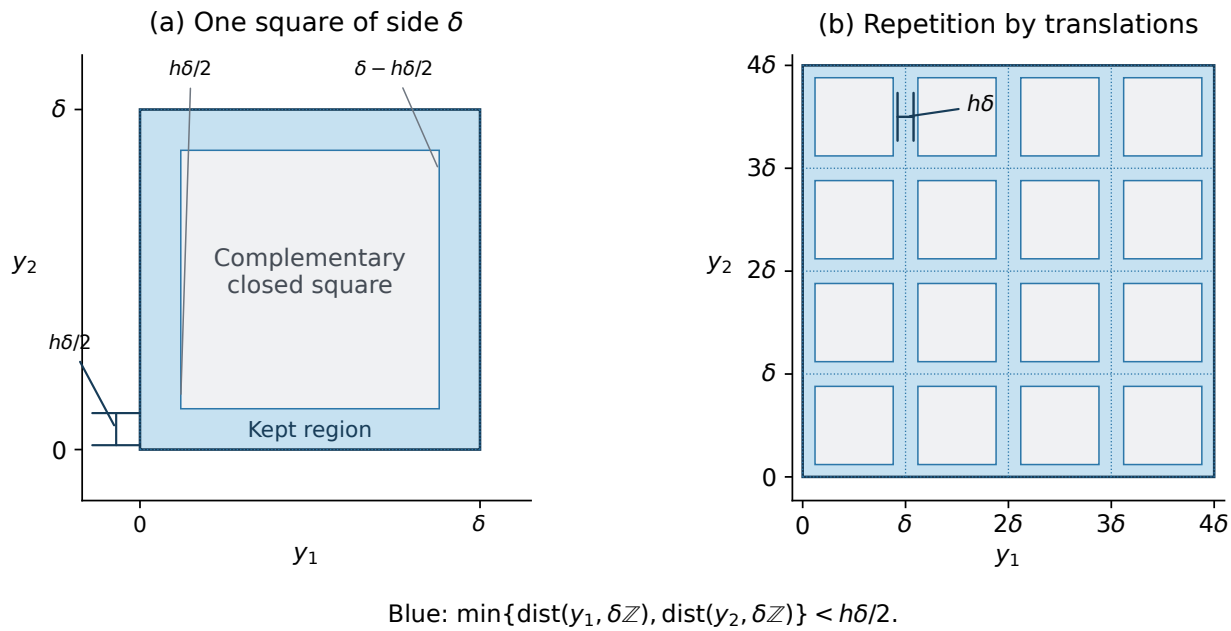

Figure 1: The set $P_{\delta,h}$ in one period and in sixteen periods. Blue is retained; grey is excluded, including its boundary. Across adjacent periods the retained strips have total width $h\delta$. For visibility the drawing uses a larger h than the parameter chosen in (3).

2.3 Six explicit coordinate maps for the sphere

Let e_1, e_2, e_3 be the standard coordinate vectors. For $i \in \{1, 2, 3\}$ and $\sigma \in \{-1, 1\}$, define the closed spherical region

$$K_{i,\sigma} = \{\omega \in S^2 : \sigma\omega_i \geq |\omega_j| \text{ for every } j \neq i\}. \tag{6}$$

These six regions cover the sphere; their interiors do not overlap. They are the radial projections of the six faces of a cube.

If $j < k$ are the other two indices, define

$$\Psi_{i,\sigma}(y_1, y_2) = \frac{\sigma e_i + y_1 e_j + y_2 e_k}{\sqrt{1 + y_1^2 + y_2^2}}, \qquad (y_1, y_2) \in [-1, 1]^2. \tag{7}$$

It maps the closed coordinate square onto $K_{i,\sigma}$. On the interiors it is smooth, one-to-one, and has the smooth inverse

$$y_1 = \frac{\omega_j}{|\omega_i|}, \qquad y_2 = \frac{\omega_k}{|\omega_i|}.$$

For example,

$$\Psi_{1,+}(y_1, y_2) = \frac{(1, y_1, y_2)}{\sqrt{1 + y_1^2 + y_2^2}}.$$

Define the set of common face boundaries by

$$\Sigma = \bigcup_{i,\sigma} \partial_{S^2} K_{i,\sigma}. \tag{8}$$

Equivalently, Σ consists of points where at least two of $|\omega_1|, |\omega_2|, |\omega_3|$ tie for the largest value. It is a finite union of great-circle arcs.

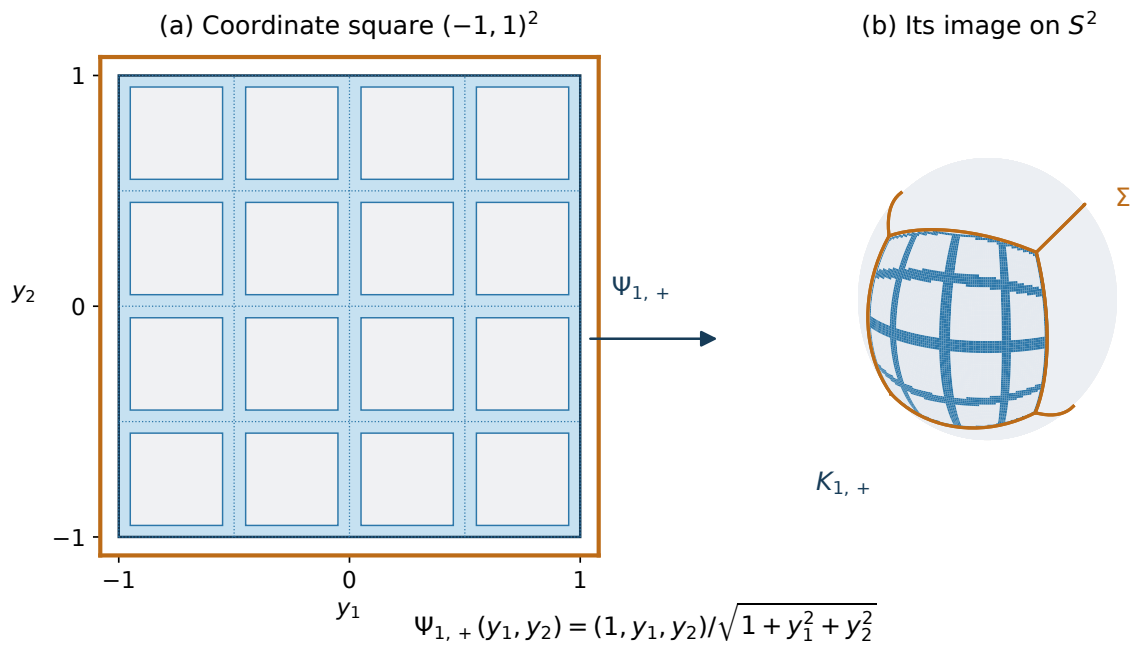

Figure 2: The explicit map $\Psi_{1,+}$ sends the square to $K_{1,+}$. Orange curves mark Σ. Blue shows the image of the planar strips on this one face; the other faces have been left plain to show the geometry. This picture illustrates the coordinate map before the boundary-neighborhood rule in the next subsection is applied.

2.4 Exactly which squares are removed from the sphere

For $\omega, \eta \in S^2$, let

$$d_{S^2}(\omega,\eta) = \arccos(\omega \cdot \eta), \qquad d_{S^2}(\omega,\Sigma) = \min_{\eta\in\Sigma} d_{S^2}(\omega,\eta).$$

These are distance along the sphere and distance to its face boundaries. Fix $M = 4$ and define the closed neighborhood

$$N_\delta = \{\omega \in S^2 : d_{S^2}(\omega,\Sigma) \le M\delta\}. \tag{9}$$

Every point of N_δ will be retained.

For each face, let $I_{i,\sigma,\delta}$ consist of the indices $a \in \mathbb{Z}^2$ for which

$$H_a \subset (-1,1)^2, \qquad \min_{y\in H_a} d_{S^2}(\Psi_{i,\sigma}(y),\Sigma) > M\delta. \tag{10}$$

Only finitely many indices satisfy this rule. Define

$$U_\delta = S^2 \setminus \bigcup_{i,\sigma} \bigcup_{a\in I_{i,\sigma,\delta}} \Psi_{i,\sigma}(H_a). \tag{11}$$

The set U_δ consists of the retained directions.

The removal rule can be read as follows. First consider all complementary squares H_a in the coordinate plane. Remove the image of such a square only when the entire square lies inside the coordinate face and its image stays farther than $M\delta$ from Σ. A square meeting the retained

boundary neighborhood is kept in its entirety. Thus no square is cut into a small fragment when two coordinate regions meet.

The removed sets are disjoint closed images of squares. In particular, U_δ is open. Its connectedness and the remaining geometric estimates are included in Lemma 1.

The construction is symmetric under $\omega \mapsto -\omega$. Indeed,

$$\Psi_{i,-}(-y) = -\Psi_{i,+}(y), \qquad -H_a = H_{-a-(1,1)},$$

and the removal rule is unchanged by this reflection. Hence $U_\delta = -U_\delta$.

2.5 From directions on the sphere to a domain in three dimensions

The final definition is

$$\Omega_\delta = B_1 \ \cup \ \{r\omega : 0 < r < R, \ \omega \in U_\delta\}. \tag{12}$$

Equivalently, a nonzero x belongs to Ω_δ exactly when

$$|x| < R \quad \text{and} \quad \big(|x| < 1 \text{ or } x/|x| \in U_\delta\big).$$

The origin belongs to the entire unit ball. The part outside the unit ball is therefore precisely

$$\{r\omega : 1 \le r < R, \ \omega \in U_\delta\}.$$

For $1 < r < R$,

$$\Omega_\delta \cap rS^2 = rU_\delta, \qquad \text{area}(rU_\delta) = r^2|U_\delta|.$$

For $r < 1$ every direction is included. At $r = 1$, the openings $\omega \in U_\delta$ are included as well.

3 The limiting eigenvalue problem

The actual eigenfunction solves a Neumann problem on Ω_δ. The limiting problem is a different variational problem on the fixed ball B_R. The precise convergence statement connecting them is Lemma 3.

3.1 Weighted norm and gradient energy

Define $m(x) = 1$ for $|x| < 1$ and $m(x) = \theta$ for $1 < |x| < R$. Its values on $|x| = 1$ do not affect any integral. For $v \in H^1(B_R)$,

$$\|v\|_m^2 = \int_{B_R} m(x)v(x)^2\,dx = \int_{B_1} v^2\,dx + \theta \int_1^R \int_{S^2} v(r,\omega)^2 r^2\,dS\,dr. \tag{13}$$

The inner product $\langle v, w\rangle_m$ is the same formula with vw instead of v^2. The word "mass" here denotes this weight in the norm.

Write $v(r,\omega) = v(r\omega)$. The derivative $\partial_r v$ measures variation along a ray. The vector $\nabla_{S^2} v(r,\omega)$ is the tangential gradient of the function $\omega \mapsto v(r\omega)$ on the unit sphere. It lies in

$$T_\omega S^2 = \{\xi \in \mathbb{R}^3 : \xi \cdot \omega = 0\}.$$

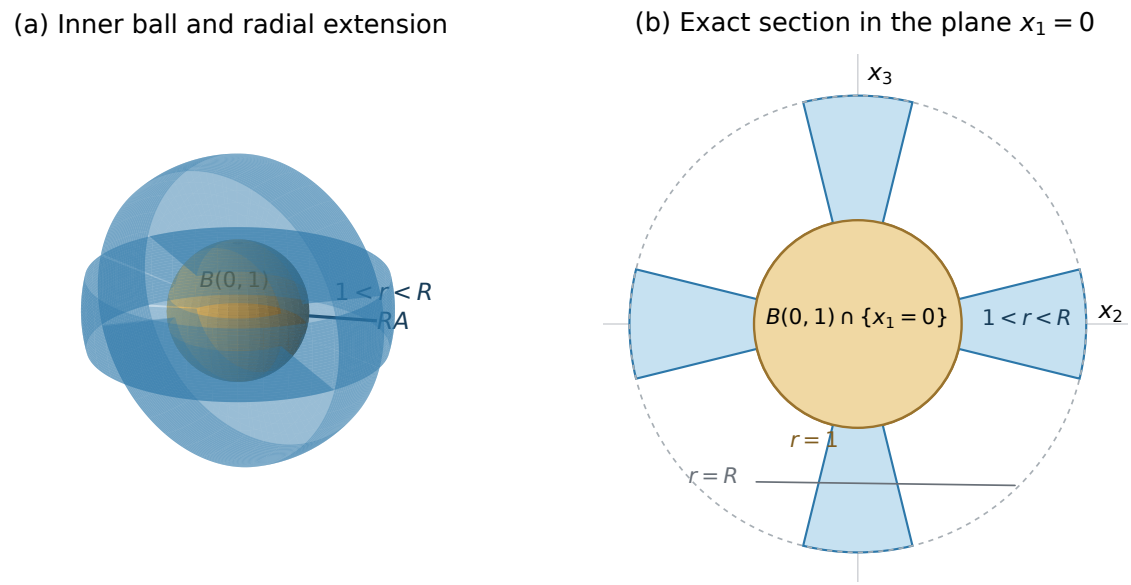

Figure 3: The radial definition illustrated with the simpler connected set $A = \{\omega : |\omega_2| < \sin(\pi/13) \text{ or } |\omega_3| < \sin(\pi/13)\}$ and $R = 2.2$. Left: transparent surfaces show $B_1 \cup \{r\omega : 0 < r < R, \omega \in A\}$. Right: its exact section in the plane $x_1 = 0$. This picture explains how angular directions are extended; the set used in the proof is the explicitly defined U_δ in (11).

For smooth v it satisfies

$$\nabla_{S^2} v(r,\omega) = r(I - \omega\omega^{\mathsf{T}})\nabla v(r\omega).$$

The limiting energy is

$$\begin{aligned}\mathcal{E}(v,v) = &\int_{B_1} |\nabla v|^2\,dx \\ &+ \int_1^R \int_{S^2} \Big[\theta r^2 |\partial_r v|^2 + \langle A(\omega)\nabla_{S^2} v, \nabla_{S^2} v\rangle\Big]\,dS\,dr.\end{aligned} \tag{14}$$

Here $A(\omega)$ is a symmetric linear map on the two-dimensional plane $T_\omega S^2$. It specifies the energy of angular variation. Section 3.2 defines it by an explicit minimization over the planar pattern. The estimates needed in the proof are

$$\frac{\theta}{6}|\xi|^2 \le \langle A(\omega)\xi,\xi\rangle \le \theta|\xi|^2, \qquad \xi \in T_\omega S^2, \tag{15}$$

uniformly in R and h. In particular, the lower comparison constant is independent of the small retained fraction θ.

The bilinear energy $\mathcal{E}(v,w)$ is obtained by replacing squares in (14) by the corresponding products. The limiting eigenproblem is

$$\mathcal{E}(v,w) = \lambda\langle v,w\rangle_m \qquad (w \in H^1(B_R)).$$

Why angular symmetry is unnecessary. We do not require $A(\omega)$ to be a scalar multiple of the identity. The weight m and the coefficient of $|\partial_r v|^2$ depend only on r, and (14) has no product between $\partial_r v$ and $\nabla_{S^2} v$. These facts let the radial and zero-spherical-average parts be treated separately in Section 5.

3.2 An explicit definition of the angular matrix

This definition specifies the coefficient A in (14). The proof in Section 5 uses only the two-sided bounds (15); its identification as the limit is proved with Lemma 3.

Use the planar set $P_{1,h}$ from (4) with $\delta = 1$, and put $Y_h = P_{1,h} \cap (0,1)^2$. The notation $H^1_{\mathrm{loc}}(P_{1,h})$ means H^1 on every open subset whose closure is a compact subset of $P_{1,h}$. Let $\mathcal{V}_h$ be the class of functions $\chi \in H^1_{\mathrm{loc}}(P_{1,h})$ such that

$$\chi(z+a) = \chi(z) \quad (a \in \mathbb{Z}^2) \quad \text{and} \quad \int_{Y_h} (|\chi|^2 + |\nabla\chi|^2)\, dz < \infty.$$

The equality expressing periodicity is understood almost everywhere. Thus the functions in this minimization have period one in the two coordinate directions. All periodicity used below is this explicit equality.

Fix a point ω in the interior of $K_{i,\sigma}$ and write $\omega = \Psi_{i,\sigma}(y)$. Let

$$F = D\Psi_{i,\sigma}(y), \qquad G = F^{\mathsf{T}} F.$$

Here F is a 3×2 matrix of derivatives; its columns span $T_\omega S^2$. The 2×2 matrix G is positive definite. For $\xi \in T_\omega S^2$, define

$$\langle A(\omega)\xi, \xi\rangle = \inf_{\chi \in \mathcal{V}_h} \int_{Y_h} \left|\xi + FG^{-1}\nabla_z \chi(z)\right|^2 dz. \tag{16}$$

The matrices F, G are held fixed at y in this minimization. The formula defines a quadratic form, and hence a symmetric map $A(\omega)$, on the tangent plane. Values on Σ may be assigned arbitrarily, since that set has surface area zero.

Meaning of the minimization. The fixed vector ξ represents a prescribed large-scale tangential gradient. The periodic function χ allows the gradient to vary within one retained planar period. The infimum is the smallest energy obtained from these variations. In the convergence proof, their scaled versions are the small within-period adjustments to the approximating functions.

The choice $\chi = 0$ gives $\langle A\xi, \xi\rangle \le \theta|\xi|^2$. A positive lower bound proportional to θ follows by integrating along the entire horizontal and vertical strips and using periodicity. The derivatives of the six maps (7) and their inverses are bounded on their closed squares, so the comparison constants are independent of h. This is the source of (15); the proof of Lemma 3 establishes this identification.

3.3 The radial equation and the interface condition

For a radial function $v(x) = f(|x|)$ define

$$p(r) = \begin{cases} r^2, & 0 < r < 1, \\ \theta r^2, & 1 < r < R. \end{cases} \tag{17}$$

Its norm and energy are $4\pi \int_0^R pf^2$ and $4\pi \int_0^R p(f')^2$. The equation is

$$-(pf')' = \lambda pf, \qquad f'(0) = f'(R) = 0. \tag{18}$$

At $r = 1$, f is continuous and

$$p(1-)f'(1-) = p(1+)f'(1+), \quad \text{equivalently} \quad f'(1-) = \theta f'(1+).$$

This is the precise meaning of "flux continuity": $4\pi pf'$ is the radial derivative multiplied by the available cross-sectional area in the weighted problem. The one-sided weighted derivatives agree at 1. Both continuity conditions follow from the variational problem on $H^1(B_R)$.

4 Auxiliary results

The six lemmas below provide the geometric, analytic, and radial estimates used in the main proof. Their proofs are given in Section 6.

Lemma 1 (Angular geometry)**.** *For the sets in (11)–(12), U_δ is open, connected, and satisfies $U_\delta = -U_\delta$. For every continuous g on S^2,*

$$\int_{U_\delta} g\, dS \longrightarrow \theta \int_{S^2} g\, dS. \tag{19}$$

The domains Ω_δ are bounded connected Lipschitz domains, starlike about 0, with

$$B_1 \subset \Omega_\delta \subset B_R, \qquad \partial\Omega_\delta \subset \{x : 1 \le |x| \le R\}.$$

For fixed R, θ, there are $c, C, a, L > 0$, independent of sufficiently small δ, such that:

- *every removed spherical square has diameter between $c\delta$ and $C\delta$, and the distance between distinct removed squares is at least $c\delta$;*
- *near every point of $\partial\Omega_\delta$, in a ball of radius $a\delta$ and suitable orthogonal coordinates, the domain is the region on one side of a graph with Lipschitz constant at most L.*

Lemma 2 (Uniform extension)**.** *For fixed R, θ, there are linear operators*

$$E_\delta : H^1(\Omega_\delta) \longrightarrow H^1(B_R)$$

such that $E_\delta v = v$ on Ω_δ and

$$\|E_\delta v\|_{H^1(B_R)} \le C\|v\|_{H^1(\Omega_\delta)}, \tag{20}$$

with C independent of δ. An extension assigns values on $B_R \setminus \Omega_\delta$ to a function initially defined on Ω_δ. The displayed inequality is the required control on those values and their gradients, including near $r = 1$ and $r = R$.

The extension estimate has two consequences used below. The extension gives the uniform Sobolev inequality

$$\|v\|_{L^6(\Omega_\delta)} \le C\big(\|\nabla v\|_{L^2(\Omega_\delta)} + \|v\|_{L^2(\Omega_\delta)}\big).$$

Here and below "uniform" means that C does not depend on δ, with R, θ fixed. Also, the extension must preserve the entire unit ball. Extending only the part in $\mathcal{A}_{1,R}$ and then attaching it to the ball can give different boundary values at $r = 1$. An extension on the whole domain avoids that mismatch. Boundary values of an H^1 function, when needed, are understood in the Sobolev sense.

Lemma 3 (Energy, eigenvalue, and eigenfunction convergence)**.** *For the geometry of Lemma 1, the actual-domain Neumann energies*

$$\mathcal{E}_\delta(v,v) = \int_{\Omega_\delta} |\nabla v|^2 \, dx$$

converge to (14)*, with mass* (13)*, as follows.*

(i) Every sequence with bounded L^2 norm and energy has an extended subsequence converging strongly in $L^2(B_R)$ to $v \in H^1(B_R)$. For every such convergent subsequence,

$$\liminf_\delta \mathcal{E}_\delta(v_\delta, v_\delta) \geq \mathcal{E}(v,v), \qquad \int_{\Omega_\delta} v_\delta^2 \, dx \longrightarrow \|v\|_m^2.$$

(ii) For every $v \in H^1(B_R)$ there is a sequence v_δ with $E_\delta v_\delta \to v$ in $L^2(B_R)$ and with convergence of its energy to $\mathcal{E}(v,v)$.

(iii) The matrix on each tangent plane satisfies (15)*; the radial coefficient is exactly θ and there is no mixed radial–angular term.*

Consequently, each indexed Neumann eigenvalue converges to the corresponding limiting eigenvalue, including multiplicities. If the limiting first positive eigenvalue is simple, the normalized first eigenfunctions on the actual domains, after a consistent choice of sign, converge after extension in $L^2(B_R)$ to the normalized limiting eigenfunction. The actual first positive eigenvalue is then simple for sufficiently small δ.

Lemma 4 (A local boundedness estimate)**.** *For fixed R, θ, there are $C, s_0 > 0$, independent of δ, with the following property. If $x \in \overline{\Omega}_\delta$, $0 < s \leq s_0$, and $v \in H^1(\Omega_\delta \cap B(x,2s))$ solves*

$$-\Delta v = F \quad \text{in } \Omega_\delta \cap B(x,2s)$$

with zero normal derivative on $\partial\Omega_\delta \cap B(x,2s)$ in the weak sense specified in Section 6.4, then, for every constant $c \in \mathbb{R}$ and $F \in L^\infty$,

$$\|v - c\|_{L^\infty(\Omega_\delta \cap B(x,s))} \leq C\Big[s^{-3/2}\|v-c\|_{L^2(\Omega_\delta \cap B(x,2s))} + s^2\|F\|_{L^\infty}\Big]. \tag{21}$$

The estimate holds also when x is near $r = 1$, near a coordinate-region boundary, or near $r = R$. Moreover, for every $\Lambda < \infty$ there is a constant $C = C(R,\theta,\Lambda)$ such that every Neumann eigenfunction normalized by $\int_{\Omega_\delta} u_\delta^2 \, dx = 1$, with eigenvalue at most Λ, satisfies

$$\|u_\delta\|_{L^\infty(\Omega_\delta)} \leq C. \tag{22}$$

Each has a continuous representative on $\overline{\Omega}_\delta$; the same local estimate holds for its boundary values.

Lemma 5 (A small radial eigenvalue)**.** *Let λ_{rad} denote the first positive eigenvalue of* (14) *restricted to radial functions. With* (3)*,*

$$\lambda_{\text{rad}} \leq CR^{-5/2} \tag{23}$$

for large R, with C independent of R.

Lemma 6 (The first radial eigenfunction)**.** *Put*

$$p(r) = r^2 \ (0 < r < 1), \qquad p(r) = \theta r^2 \ (1 < r < R).$$

The first positive radial eigenvalue is simple. A corresponding real eigenfunction f, chosen with $f(0) > 0$, has exactly one zero in $(0, R)$, has weighted mean zero, and satisfies (18) with equal one-sided values of pf' at $r = 1$. In the unit ball,

$$f(r) = f(0)\frac{\sin(\sqrt{\lambda}\, r)}{\sqrt{\lambda}\, r}, \tag{24}$$

with the value at $r = 0$ understood by continuity.

5 Proof of the main theorem

We prove more precisely that, for all sufficiently large fixed R and then all sufficiently small δ, the domains Ω_δ defined in (12) satisfy every conclusion of Theorem 1.

5.1 The first limiting eigenfunction is radial

For $v \in H^1(B_R)$, define its spherical average

$$\bar{v}(r) = \frac{1}{4\pi}\int_{S^2} v(r,\omega)\, dS, \qquad v^\perp = v - \bar{v}.$$

Spherical averaging is a bounded projection on $H^1(B_R)$: Jensen's inequality controls its L^2 norm and radial derivative, and its angular derivative vanishes. It also preserves the weighted mean. Thus $v^\perp$ has zero spherical average for almost every r. Radial functions and these mean-zero functions are orthogonal for both the mass inner product and the energy. For the radial energy term, the cross term vanishes because $\int_{S^2} \partial_r v^\perp\, dS = 0$; for the angular term, it vanishes because $\nabla_{S^2}\bar{v} = 0$. The same statements hold in the ball.

Consequently eigenvalue minimization can be carried out separately among radial functions and among functions with zero spherical average, even when $A(\omega)$ depends on the angular direction. For the latter functions, the spherical Poincaré inequality is

$$\int_{S^2} |\nabla_{S^2} v^\perp|^2\, dS \geq 2\int_{S^2} |v^\perp|^2\, dS.$$

For $0 < r < 1$, $r^2 \leq 1$; for $1 < r < R$, $r^2 \leq R^2$. With (15), this gives

$$\mathcal{E}(v^\perp, v^\perp) \geq \frac{1}{3R^2}\|v^\perp\|_m^2. \tag{25}$$

Lemma 5 gives $\lambda_{\text{rad}} \leq CR^{-5/2}$. Choose R so large that

$$CR^{-5/2} < \frac{1}{3R^2}.$$

The first positive limiting eigenvalue is therefore $\lambda = \lambda_{\text{rad}}$. It is simple by Lemma 6, and its eigenfunction $u_0(x) = f(|x|)$ is radial. Normalize it by $\|u_0\|_m = 1$ and $f(0) > 0$.

5.2 Strict radial decrease

Let $z \in (0, R)$ be its unique zero. Then $f > 0$ before z and $f < 0$ after z. Define

$$J(r) = \int_0^r p(s) f(s)\, ds.$$

For $0 < r \le z$, $J(r) > 0$. For $z < r < R$, the weighted mean-zero property gives

$$J(r) = -\int_r^R p(s) f(s)\, ds > 0.$$

Integrating (18) from 0 to r, using $pf' \to 0$ at 0 and equality of the one-sided weighted derivatives at 1, gives

$$p(r) f'(r) = -\lambda J(r) < 0 \qquad (0 < r < R). \tag{26}$$

Thus f is strictly decreasing, with one-sided derivatives at 1. In particular,

$$G = f(0) - f(1) > 0, \qquad \sup_{1 \le r \le R} f(r) = f(1). \tag{27}$$

Here R is fixed, so the positive number G is independent of δ.

5.3 Eigenvalue and eigenfunction convergence

By Lemma 3, for sufficiently small δ the first positive actual-domain eigenvalue λ_δ is simple and tends to λ. Choose its real eigenfunction u_δ with

$$\int_{\Omega_\delta} u_\delta\, dx = 0, \qquad \int_{\Omega_\delta} u_\delta^2\, dx = 1,$$

and choose its sign to converge to u_0. Put

$$\eta_\delta = \|E_\delta u_\delta - u_0\|_{L^2(B_R)} \longrightarrow 0.$$

The eigenvalues are bounded and Lemma 4 supplies a uniform bound on $\|u_\delta\|_\infty$. Hence

$$F_\delta = \lambda_\delta u_\delta$$

is bounded in L^∞, independently of δ.

5.4 Uniform convergence on the actual domains

Define

$$\omega_0(t) = \sup\{|u_0(x) - u_0(y)| : x, y \in \overline{B}_R,\ |x - y| \le t\}.$$

Since u_0 is continuous on the compact ball, $\omega_0(t) \to 0$ as $t \downarrow 0$. Fix $s \in (0, s_0]$.

For any $x \in \overline{\Omega}_\delta$, apply (21) to $v = u_\delta$ and the *constant* $c = u_0(x)$. In $\Omega_\delta \cap B(x, 2s)$,

$$\begin{aligned} \|u_\delta - u_0(x)\|_{L^2} &\le \|u_\delta - u_0\|_{L^2} + \|u_0 - u_0(x)\|_{L^2} \\ &\le \eta_\delta + C s^{3/2} \omega_0(2s). \end{aligned}$$

The local estimate therefore gives, with a new constant C,

$$\sup_{x\in\overline{\Omega}_\delta} |u_\delta(x) - u_0(x)| \le C\Big[s^{-3/2}\eta_\delta + \omega_0(2s) + s^2\Big]. \tag{28}$$

First let $\delta \downarrow 0$ with s fixed; then let $s \downarrow 0$. It follows that

$$\sup_{x\in\overline{\Omega}_\delta} |u_\delta(x) - u_0(x)| \longrightarrow 0. \tag{29}$$

The use of a constant preserves the zero normal derivative: $u_\delta - u_0(x)$ has the same boundary condition as u_δ. The estimate is applied on the actual domain, including its boundary.

5.5 The strict boundary gap

Take δ so small that the error in (29) is less than $G/4$. Lemma 1 and (27) give

$$u_0(x) \le f(1) = f(0) - G \qquad (x \in \partial\Omega_\delta).$$

Therefore

$$u_\delta(0) \ge f(0) - G/4, \qquad \max_{\partial\Omega_\delta} u_\delta \le f(0) - 3G/4.$$

This proves (2), with a gap at least $G/2$.

5.6 The unique maximum is at the origin

Because $\Omega_\delta = -\Omega_\delta$, the function $u_\delta(-x)$ is another eigenfunction for the same simple eigenvalue. Thus it equals either $u_\delta(x)$ or $-u_\delta(x)$. For small δ, (29) gives $u_\delta(0) > 0$, which excludes the minus sign. Hence u_δ is even and

$$\nabla u_\delta(0) = 0.$$

Put $w_\delta = u_\delta - u_0$. On the fixed ball B_1,

$$-\Delta w_\delta = \lambda_\delta w_\delta + (\lambda_\delta - \lambda)u_0.$$

Choose fixed $0 < \rho < \rho_1 < \rho_2 < 1$. The interior H^2 estimate for the Laplacian gives

$$\|w_\delta\|_{H^2(B_{\rho_1})} \le C\big(\|w_\delta\|_{L^2(B_{\rho_2})} + |\lambda_\delta - \lambda|\big) \longrightarrow 0.$$

The corresponding estimate for two more derivatives, on the smaller ball, gives

$$\|w_\delta\|_{H^4(B_\rho)} \le C\big(\|w_\delta\|_{H^2(B_{\rho_1})} + |\lambda_\delta - \lambda|\big) \longrightarrow 0.$$

Here u_0 is smooth in B_1 and the eigenvalues are bounded. In dimension three, $H^4(B_\rho)$ embeds continuously into $C^2(\overline{B}_\rho)$, so

$$u_\delta \longrightarrow u_0 \quad \text{in } C^2(\overline{B}_\rho) \qquad (\rho < 1).$$

Formula (24) gives

$$D^2 u_0(0) = -\frac{\lambda f(0)}{3} I.$$

Choose $0 < \rho < 1$ and $a > 0$ so that $D^2 u_0 \le -2aI$ throughout $\overline{B}_\rho$. For sufficiently small δ, $D^2 u_\delta \le -aI$ there. Since $\nabla u_\delta(0) = 0$,

$$u_\delta(x) \le u_\delta(0) - \frac{a}{2}|x|^2 \qquad (0 < |x| \le \rho).$$

On the rest of the domain, strict radial decrease gives the fixed gap

$$H = f(0) - f(\rho) > 0.$$

Take the uniform error in (29) smaller than $H/3$. For $|x| \ge \rho$,

$$u_\delta(x) \le f(\rho) + H/3 = f(0) - 2H/3 < u_\delta(0).$$

Combining the two regions proves (1) and completes the proof. □

6 Proofs of the auxiliary results

We use standard extension, trace, Sobolev, compactness, and Poincaré results on fixed bounded Lipschitz domains; see [21, 11]. The constructions below establish the estimates uniform in δ that are needed here. We also use the variational characterization of Neumann eigenvalues, the spherical Poincaré inequality with constant 2, and interior elliptic estimates. Boundary continuity follows from [17, Proposition 3.6], as used in Section 6.4.

6.1 Proof of Lemma 1

Throughout this proof R and h are fixed. All constants may depend on them, but not on δ. Put $Q = (0,1)^2$ and

$$H = [h/2, 1 - h/2]^2, \qquad Y = Q \setminus H, \qquad Q_a = \delta(a + Q).$$

Thus $H_a = \delta(a + H)$. The six maps $\Psi_{i,\sigma}$ and their inverses have uniformly bounded first derivatives on their closed coordinate squares. Consequently there are absolute constants $b_0, b_1 > 0$ such that

$$b_0|y - z| \le d_{S^2}(\Psi_{i,\sigma}(y), \Psi_{i,\sigma}(z)) \le b_1|y - z| \qquad (y, z \in [-1,1]^2). \tag{30}$$

For the upper bound one can take $b_1 = 1$: the norm of $D\Psi$ is at most 1, and the image of the straight segment from y to z has length at most $|y - z|$. The lower bound follows, for example, from the displayed inverse formula and $|\omega_i| \ge 1/\sqrt{3}$ on the face.

Every selected H_a is at spherical distance greater than 4δ from Σ. Its surrounding entire period square $\overline{Q}_a$ is still inside the coordinate face. Indeed, every point of $\overline{Q}_a$ is at Euclidean distance at most $h\delta/\sqrt{2}$ from H_a. If $\overline{Q}_a$ crossed a face boundary, the line segment from H_a to the first boundary point, followed by Ψ, would contradict the 4δ distance condition. In particular,

$$d_{S^2}(\Psi(\overline{Q}_a), \Sigma) > 3\delta. \tag{31}$$

The images of these surrounding period squares have disjoint interiors on each face, and they are disjoint across different faces. This additional observation will be useful for the extension proof.

The removed sets are finitely many disjoint closed topological disks. Their diameters lie between $b_0(1-h)\delta$ and $b_1\sqrt{2}(1-h)\delta$. On the same face, distinct squares have coordinate distance at least $h\delta$,

so their spherical distance is at least $b_0 h\delta$. For squares on distinct faces, every path from one to the other crosses Σ, and their distance is greater than 8δ. Thus the asserted separation estimate holds. Their complement is open and connected. To verify connectedness directly, join two points of the complement by a path on the sphere. Enlarge each removed square slightly to a closed concentric square H_a^+, still within its face, such that the enlarged images are mutually disjoint and contain neither endpoint. This is possible by separation and the positive distance of each endpoint from the finitely many removed sets. Whenever the path enters the image of H_a^+, replace the portion between its first and last intersections with that image by a path along $\Psi(\partial H_a^+)$. This curve lies entirely in U_δ. The enlarged images are disjoint, so a replacement cannot meet another removed set. There are only finitely many disks, and these replacements give a path in U_δ. Antipodal symmetry follows from the two identities for Ψ and H_a already displayed in the construction.

Here is the averaging argument, including the effect of the removal rule. In each coordinate square the ordinary repeated pattern has indicator $\mathbf{1}_Y(y/\delta)$, interpreted periodically. For every continuous f on $[-1,1]^2$,

$$\int_{[-1,1]^2} f(y)\mathbf{1}_Y(y/\delta)\,dy \longrightarrow \theta \int_{[-1,1]^2} f(y)\,dy. \tag{32}$$

To prove this, sum over the whole period squares contained in $[-1,1]^2$. On each such square subtract the value of f at one point. The error is at most its area times the modulus of continuity of f at $\sqrt{2}\delta$. The squares intersecting the boundary have total area $O(\delta)$. The integral of the periodic indicator on a whole square is exactly $\theta\delta^2$, which proves (32).

A complementary square not removed by the rule either intersects the boundary of its face or has an image meeting $\{d_{S^2}(\omega,\Sigma) \le 4\delta\}$. Its whole image is therefore within distance $(4+\sqrt{2})\delta$ of Σ, by (30). The face-boundary squares satisfy the same type of bound. Since Σ is a finite union of smooth arcs, this neighborhood has area $O(\delta)$: an arc of length ℓ has a neighborhood of width t with area at most $C(\ell t + t^2)$, as is seen by covering it with consecutive geodesic rectangles and two end disks. In (32) take

$$f(y) = g(\Psi(y))J(y), \qquad J(y) = (1+y_1^2+y_2^2)^{-3/2},$$

and sum over the six faces. The retained extra neighborhood has vanishing area. This proves (19).

The domain formula immediately shows that Ω_δ is open, bounded, starlike, and contains B_1. Any point can be joined to 0 by its radial segment, so the domain is connected. Its boundary can contain no point with $|x| < 1$ or $|x| > R$, proving the asserted boundary inclusion.

For clarity, we give the local boundary check rather than inferring it from openness. Inside one face, a removed set is bounded by four planes through 0: an edge $y_1 = c$ becomes $x_j = c\sigma x_i$, and an edge $y_2 = c$ becomes $x_k = c\sigma x_i$. Its two radial ends are the spheres $r = 1$ and $r = R$. Near a corner at the lower end, suitable signed coordinates (s, z_1, z_2) make the removed set

$$\{s \ge 0,\ z_1 \ge 0,\ z_2 \ge 0\}.$$

Here $s = r - 1$; one or both z inequalities are omitted at an edge or in the relative interior of a face. The domain is the complement of this orthant. At the upper end, with $s = R - r$, the corresponding domain is

$$\{s > 0\} \cap \big(\{z_1 < 0\} \cup \{z_2 < 0\}\big).$$

Again one inequality is omitted when only one edge is present. Away from the ends the same models have an unrestricted s.

All these models are Lipschitz graph domains. More explicitly, in coordinates $q = t(1,1,1)/\sqrt{3}+z$ with $z_1 + z_2 + z_3 = 0$, the complement of the positive orthant is

$$t < \max_i(-\sqrt{3}z_i).$$

The upper-end model, after reversing the signs of the last two coordinates, is an intersection of one positive half-space and the union of two positive half-spaces; in the same diagonal coordinates its graph is explicitly

$$t > \max\big(-\sqrt{3}z_1, \min(-\sqrt{3}z_2, -\sqrt{3}z_3)\big).$$

Maxima and minima preserve the Lipschitz bound of these affine functions. The two-dimensional edge models are the corresponding formulas with two coordinates.

The actual coordinates $(r, y_1, y_2) \mapsto r\Psi(y)$ are smooth with bounded invertible derivative for $1/2 \le r \le R+1$. On a neighborhood of diameter $O(\delta)$ their derivative differs from its value at the center by $O(\delta)$, uniformly. A linear invertible image of any of the preceding graph models is a graph in the direction which is the image of its original graph direction, with a bound depending only on the derivative and its inverse. The $O(\delta)$ perturbation retains this property for sufficiently small δ. To check the last assertion, project the perturbed boundary onto the plane perpendicular to this direction. The projection is the sum of an invertible linear map and a map with Lipschitz norm $O(\delta)(1 + L_0)$, where L_0 is the model graph bound. Its inverse and the height function are therefore Lipschitz with uniform bounds.

Choose $a > 0$ smaller than a fixed multiple of both h and $1 - h$. The identity $|r\omega - s\eta|^2 = (r-s)^2 + rs|\omega - \eta|^2$, for $r, s \ge 1$, transfers the angular separation estimate to the excluded radial sets. Thus a ball of radius $a\delta$ meets at most one removed square, and cannot meet two opposite edges of that square. Choose also δ small enough that it cannot meet both radial ends. It thus has one of the graph models just listed. Near Σ no removed square is present by (31); only the smooth outer sphere can be a boundary there. This proves the quantified Lipschitz statement and completes the geometry lemma. □

6.2 Proof of Lemma 2

We construct the operator. An angular extension used separately above $r = 1$ would not preserve the trace of the function on the unit sphere. The following construction includes a three-dimensional extension on a layer of thickness δ at this interface.

We first record precisely the two fixed-domain operators used. Besides Q, H, Y above, define the open three-dimensional set

$$D = \big((-1,0) \times Q\big) \ \cup \ \big((-1,2) \times Y\big), \qquad F = (-1,2) \times Q. \tag{33}$$

There are linear operators $T : H^1(Y) \to H^1(Q)$ and $S : H^1(D) \to H^1(F)$, equal to their input on its original set, preserving constants, and satisfying

$$\|Tu\|_{L^2(Q)} \le C_h \|u\|_{L^2(Y)}, \qquad \|\nabla Tu\|_{L^2(Q)} \le C_h \|\nabla u\|_{L^2(Y)}, \tag{34}$$

$$\|Su\|_{L^2(F)} \le C_h \|u\|_{L^2(D)}, \qquad \|\nabla Su\|_{L^2(F)} \le C_h \|\nabla u\|_{L^2(D)}. \tag{35}$$

Both Y and D are fixed bounded connected Lipschitz domains; their corner geometry was checked above. The fixed-domain extension theorem and its reflection construction [21, Theorem 5.2.1 and

its proof] give, for either source G, a linear extension A into the surrounding rectangle with

$$\|Au\|_2 \le C_h\|u\|_2, \qquad \|\nabla Au\|_2 \le C_h(\|\nabla u\|_2 + \|u\|_2). \tag{36}$$

The separate L^2 bound follows from the same reflection and partition of unity, without differentiating. If u_G is the mean of u on G, the Poincaré inequality [21, Theorem 7.1.1] gives $\|u-u_G\|_2 \le C_h\|\nabla u\|_2$. Thus replacing A by $u \mapsto A(u-u_G)+u_G$ preserves the extension property and the L^2 bound, preserves constants, and removes the $\|u\|_2$ term from the gradient bound. This proves (34)–(35). In particular, T is bounded on L^2 and hence commutes with weak radial differentiation, by difference quotients:

$$\partial_r(Tu) = T(\partial_r u). \tag{37}$$

We now apply these fixed operators to each selected square. Fix one such square on one face and suppress its face index. Use coordinates

$$x = r\Psi(y), \qquad y = \delta(a+z), \quad z \in Q.$$

For $r \ge 1$, the source over this period is precisely $z \in Y$. For $r < 1$ the whole period is in the domain. Write $\hat{v}(r,y) = v(r\Psi(y))$. Let $b_a(r,y)$ be the scaled angular extension T of $\hat{v}(r,\cdot)$, for $1 < r < R$. For $1-\delta < r < 1+2\delta$, let $s_a(r,y)$ be the scaled three-dimensional extension S under

$$t = (r-1)/\delta, \qquad z = y/\delta - a.$$

Its source is exactly the image of D in (33). For all sufficiently small δ this image lies inside B_R. By (31), it meets no other removed set.

Fix a smooth function χ on $\mathbb{R}$ with $0 \le \chi \le 1$, $\chi(t) = 1$ for $t \le 1$, and $\chi(t) = 0$ for $t \ge 3/2$. The function χ is a cutoff: in the formula below it selects s_a for $r \le 1+\delta$ and b_a for $r \ge 1+3\delta/2$. On the excluded set associated with H_a, define

$$(E_\delta v)(r\Psi(y)) = \begin{cases} \chi((r-1)/\delta)s_a(r,y) + (1-\chi((r-1)/\delta))b_a(r,y), & 1 \le r < 1+2\delta, \\ b_a(r,y), & 1+2\delta \le r < R. \end{cases} \tag{38}$$

On Ω_δ itself set $E_\delta v = v$. Because both local operators equal the input on Y, the formulas have the original trace on every lateral edge. At $r = 1$ the cutoff is 1, and S equals v throughout the lower half of its box; hence it gives exactly the unit-ball trace. In fact near the outer edges of each period square the result equals v on an open strip, since H_a is inset by $h\delta/2$. Thus different period definitions glue without a jump. At $r = R$ no further gluing is needed: the target space is $H^1(B_R)$. These observations and the trace gluing rule for H^1 functions prove that the result belongs to $H^1(B_R)$. The entire unit ball is preserved.

We give the uniform estimates, including the term created by the cutoff. In these coordinates

$$dx = r^2 J(y)\, dr\, dy,$$

and the gradient norm is uniformly equivalent, for fixed R and $1/2 < r < R$, to

$$\int (|\partial_r \hat{v}|^2 + |\nabla_y \hat{v}|^2)\, dr\, dy.$$

All equivalence constants are independent of δ and a. Scaling (34) and using (37) give

$$\int_{Q_a} |b_a|^2\,dy \le C_h \int_{Q_a\setminus H_a} |\hat{v}|^2\,dy,$$
$$\int_{Q_a} |\nabla_y b_a|^2\,dy \le C_h \int_{Q_a\setminus H_a} |\nabla_y \hat{v}|^2\,dy,$$
$$\int_{Q_a} |\partial_r b_a|^2\,dy \le C_h \int_{Q_a\setminus H_a} |\partial_r \hat{v}|^2\,dy.$$

The scaled S has the same L^2 and full-gradient bounds on its three-dimensional box, because all three coordinates are scaled by δ.

Let D_a denote its source box in (r, y) coordinates, and let c_a be the ordinary coordinate mean of $\hat{v}$ on D_a. Its scaled Poincaré inequality reads

$$\int_{D_a} |\hat{v} - c_a|^2\,dr\,dy \le C_h\delta^2 \int_{D_a} (|\partial_r \hat{v}|^2 + |\nabla_y \hat{v}|^2)\,dr\,dy.$$

Since S and T preserve constants and are L^2 bounded, on the transition box $1+\delta < r < 1+3\delta/2$ this implies

$$\int |s_a - b_a|^2\,dr\,dy \le C_h\delta^2 \int_{D_a} (|\partial_r \hat{v}|^2 + |\nabla_y \hat{v}|^2)\,dr\,dy. \tag{39}$$

The extra derivative in (38) is $\delta^{-1}\chi'((r-1)/\delta)(s_a - b_a)$. Equation (39) bounds its squared integral by the source energy, with no negative power of δ remaining.

The angular period interiors are disjoint, including across faces. The source sets D_a are therefore disjoint as well. Within each period the angular and bottom source estimates overlap at most twice. Summing the estimates and adding the unchanged part of the domain proves the stronger pair of bounds

$$\|E_\delta v\|_{L^2(B_R)} \le C_{R,h}\|v\|_{L^2(\Omega_\delta)}, \qquad \|\nabla E_\delta v\|_{L^2(B_R)} \le C_{R,h}\|\nabla v\|_{L^2(\Omega_\delta)}. \tag{40}$$

This proves (20). Applying the ordinary Sobolev inequality on the fixed ball to $E_\delta v$ gives the stated uniform L^6 inequality on Ω_δ.

□

6.3 Proof of Lemma 3

Fix R and h. Compactness and approximation constants may depend on them; the bounds on A/θ below do not.

1. Coordinates and the exact energy formula. Put $Q = (-1,1)^2$, $Y = (0,1)^2$, and

$$Y_h = P_{1,h} \cap Y, \qquad \chi_h = \mathbf{1}_{P_{1,h}}.$$

The function χ_h is regarded as a function of period 1 in each coordinate. Its average over Y is θ. On one of the six spherical regions, suppress the two face indices and write

$$F(y) = D\Psi(y), \quad G(y) = F(y)^\mathsf{T} F(y), \quad J(y) = \sqrt{\det G(y)}, \quad X(r,y) = r\Psi(y).$$

The functions G, G^{-1}, J, J^{-1} are smooth and bounded on $\overline{Q}$, uniformly over the six faces. For $w = v \circ X$, orthogonality of Ψ to the columns of F gives

$$dx = r^2 J(y)\, dr\, dy, \qquad |\nabla v(X(r,y))|^2 = |\partial_r w|^2 + r^{-2}(\nabla_y w)^{\mathsf{T}} G(y)^{-1} \nabla_y w. \tag{41}$$

In particular, $\nabla_{S^2} v = F G^{-1} \nabla_y w$.

For every compact subset $Q' \subset Q$, the retained set in these coordinates is, for all sufficiently small δ, exactly

$$\mathbf{1}_{U_\delta}(\Psi(y)) = \chi_h(y/\delta) \qquad (y \in Q'). \tag{42}$$

Indeed, every complementary square meeting Q' eventually satisfies the removal rule. The additionally retained part lies within distance $C\delta$ of ∂Q and has spherical area $O(\delta)$. Periodic averaging, first for continuous tests and then by L^1 approximation, therefore gives

$$\mathbf{1}_{\Omega_\delta} \overset{*}{\rightharpoonup} m \quad \text{in } L^\infty(B_R). \tag{43}$$

2. The cell minimization and its bounds. For a positive definite 2×2 matrix D and $\eta \in \mathbb{R}^2$, put

$$B(D, \eta) = \min_{\zeta \in \mathcal{V}_h} \int_{Y_h} (\eta + \nabla_z \zeta)^{\mathsf{T}} D (\eta + \nabla_z \zeta)\, dz. \tag{44}$$

On the connected Lipschitz set Y_h, impose equal traces on opposite outside edges and $\int_{Y_h} \zeta = 0$. These define a closed subspace of $H^1(Y_h)$. Poincaré's inequality and the Lax–Milgram theorem [11] give a unique minimizer, characterized by

$$\int_{Y_h} \nabla \varphi^{\mathsf{T}} D (\eta + \nabla \zeta)\, dz = 0 \qquad (\varphi \in \mathcal{V}_h). \tag{45}$$

The minimizer depends linearly on η. Filling the central square by a bounded H^1 extension leaves the outside-edge traces unchanged, and hence extends cell functions to $H^1_{\mathrm{per}}(Y)$. Periodic convolution then gives density of smooth periodic restrictions in $\mathcal{V}_h$. This fixed-cell extension may depend on h.

If $d_- I \le D \le d_+ I$, the following elementary estimates hold:

$$d_- h |\eta|^2 \le B(D, \eta) \le \theta \eta^{\mathsf{T}} D \eta. \tag{46}$$

For the lower bound, fix z_2 in the horizontal strip, of total width h. Periodicity gives

$$\int_0^1 (\eta_1 + \partial_{z_1} \zeta)\, dz_1 = \eta_1,$$

so Cauchy–Schwarz gives an integral of its square at least η_1^2. Integrating in this strip gives $h\eta_1^2$. The vertical strip gives $h\eta_2^2$ for the other component. These two estimates can be added because they concern the two different components of $|\eta + \nabla\zeta|^2$, even in their overlap. Multiply by d_- and take the infimum. The upper bound uses $\zeta = 0$. The argument holds for all H^1 cell functions by Fubini and their periodic trace values.

For a tangent vector ξ at $\omega = \Psi(y)$ put $\eta = F(y)^{\mathsf{T}} \xi$. Then $F G^{-1} \eta = \xi$, and the definition in Section 3.2 is precisely

$$\xi^{\mathsf{T}} A(\omega) \xi = B(G(y)^{-1}, \eta). \tag{47}$$

For completeness, this gives the explicit constants in (15). Put $s = |y|^2$. Direct differentiation of (7) gives

$$G = (1+s)^{-1} I - (1+s)^{-2} y y^{\mathsf{T}}.$$

Its eigenvalues are $(1+s)^{-1}$ and $(1+s)^{-2}$, so those of G^{-1} are $1+s$ and $(1+s)^2$. Using (46) and $|\xi|^2 = \eta^{\mathsf{T}} G^{-1} \eta$, we obtain

$$\xi^{\mathsf{T}} A(\omega) \xi \geq h(1+s)|\eta|^2 \geq \frac{h}{1+s}|\xi|^2 \geq \frac{\theta}{6}|\xi|^2.$$

Here $s \leq 2$ and $h \geq \theta/2$. The upper bound is $\xi^{\mathsf{T}} A(\omega)\xi \leq \theta|\xi|^2$, by the zero cell function. Both constants are independent of h and R.

Write $\zeta(D, \eta)$ for the normalized minimizer. Subtracting two instances of (45) and testing with the difference of the minimizers gives, on compact sets of positive definite matrices,

$$\|\nabla\zeta(D,\eta) - \nabla\zeta(\widetilde{D},\widetilde{\eta})\|_2 \leq C\big(|\eta - \widetilde{\eta}| + |D - \widetilde{D}|\,|\widetilde{\eta}|\big).$$

By Poincaré, this also gives H^1 continuity. Thus A is continuous within each face and measurable on the sphere; its values on the face boundaries are irrelevant.

3. Compactness and convergence of the norm. For v_δ with bounded norm and energy, Lemma 2 and Rellich compactness give, along a subsequence, $\widetilde{v}_\delta = E_\delta v_\delta \rightharpoonup v$ in $H^1(B_R)$ and $\widetilde{v}_\delta \to v$ in $L^2(B_R)$. Hence $\widetilde{v}_\delta^2 \to v^2$ in L^1, and (43) gives

$$\int_{\Omega_\delta} v_\delta^2 \, dx \longrightarrow \int_{B_R} m v^2 \, dx. \tag{48}$$

Polarization gives convergence of the corresponding inner products. Recall that $m \geq \theta > 0$.

4. What the gradients can do within a period. We give the needed partial unfolding argument; see [8] for the general method. Here $H^1_{\mathrm{per}}(Y)$ consists of $H^1(Y)$ functions with equal opposite-edge traces.

Suppose w_δ is bounded in $H^1(I \times Q)$, where I is a bounded interval, and $w_\delta \to w$ in L^2. For every square $\delta(a + Y)$ contained in Q, and every y in that square, define

$$T_\delta f(r, y, z) = f(r, \delta a + \delta z), \qquad z \in Y.$$

Set $T_\delta f = 0$ outside the union Q_δ of these squares. Change of variables gives

$$\int_{I \times Q \times Y} |T_\delta f|^2 \, dr\, dy\, dz = \int_{I \times Q_\delta} |f|^2 \, dr\, dy.$$

Thus T_δ is an L^2 contraction. By continuous approximation, $T_\delta w \to w$, so also $T_\delta w_\delta \to w$ strongly in L^2. Extract weak L^2 limits q_r, q_y of the unfolded derivatives.

For smooth compactly supported $\varphi(r, y)$ and smooth periodic $\psi(z)$,

$$\int_{I \times Q} f_\delta(r, y)\varphi(r, y)\psi(y/\delta)\, dr\, dy \longrightarrow \int_{I \times Q \times Y} q(r, y, z)\varphi(r, y)\psi(z)\, dr\, dy\, dz \tag{49}$$

whenever f_δ is bounded in L^2 and $T_\delta f_\delta \rightharpoonup q$. Indeed, freezing φ within each square introduces an error at most $C\delta\|f_\delta\|_2$; the omitted boundary region contributes at most $C|Q \setminus Q_\delta|^{1/2}\|f_\delta\|_2$. This also proves periodic averaging, with integrable periodic factors handled by $L^1(Y)$ approximation.

Integration by parts gives

$$\int \partial_r w_\delta \, \varphi \, \psi(y/\delta) = -\int w_\delta \, \partial_r \varphi \, \psi(y/\delta).$$

Strong L^2 convergence, periodic averaging, and (49) yield

$$q_r(r, y, z) = \partial_r w(r, y). \tag{50}$$

For the angular derivatives, constant ψ first gives

$$\int_Y q_y(r, y, z) \, dz = \nabla_y w(r, y).$$

For periodic vector fields with $\operatorname{div}_z \psi = 0$, integration by parts has no δ^{-1} term:

$$\int \nabla_y w_\delta \cdot \varphi\psi(y/\delta) = -\int w_\delta \, \nabla_y \varphi \cdot \psi(y/\delta).$$

Passing to the limit shows that $b = q_y - \nabla_y w$ is orthogonal in the periodic variable to every divergence-free field. Its Fourier coefficients satisfy $\widehat{b}(0) = 0$ and $\widehat{b}(k) \parallel k$ for $k \neq 0$. Define W by

$$\widehat{W}(k) = \frac{k \cdot (\widehat{q_y - \nabla_y w})(k)}{2\pi i |k|^2}, \quad (k \neq 0), \qquad \widehat{W}(0) = 0.$$

Parseval's identity gives $W \in L^2(I \times Q; H^1_{\mathrm{per}}(Y))$ and

$$q_y = \nabla_y w + \nabla_z W. \tag{51}$$

A countable family of Fourier tests establishes these identities for almost every (r, y); the formula also gives measurability of W.

5. The lower energy bound. Compose the extended functions $\widetilde{v}_\delta$ with $X(r, y)$ on each face. Formula (41) shows that the resulting functions are bounded in $H^1((1, R) \times Q)$ and converge strongly in L^2 to $w = v \circ X$. Fix a smaller rectangle $Q' \subset Q$ and a smaller interval $I \subset (1, R)$. For small δ, (42) holds on this rectangle. Unfold the exact annular energy there. On every complete period square its indicator becomes exactly $\chi_h(z)$.

Replacing the smooth coefficients evaluated at $\delta a + \delta z$ by their values at y changes the energy by $o(1)$, since the gradients are uniformly bounded in L^2. Omit squares cut by $\partial Q'$, whose energy is nonnegative. Weak lower semicontinuity and (50)–(51) give

$$\begin{aligned} \liminf_{\delta \to 0} \int_{\Omega_\delta \cap X(I \times Q')} |\nabla v_\delta|^2 \, dx \geq \int_{I \times Q' \times Y_h} J(y) \Big[& r^2 |\partial_r w|^2 \\ & + (\nabla_y w + \nabla_z W)^{\mathsf{T}} G(y)^{-1} (\nabla_y w + \nabla_z W) \Big] \, dr \, dy \, dz. \end{aligned} \tag{52}$$

This follows first on rectangles a positive distance inside Q', and then on Q' by exhaustion; no bound on the discarded energy is needed.

At almost every (r, y), the restriction of W to Y_h is an admissible periodic cell function. Minimizing its angular contribution in (52), and integrating the radial contribution over Y_h, gives

$$\int_{I\times Q'} J(y)\Big[\theta r^2|\partial_r w|^2 + B(G(y)^{-1}, \nabla_y w)\Big]\, dr\, dy.$$

Use (47) and $dS = J(y)dy$, exhaust the interval and six open faces, and add the weak lower bound in B_1. This proves

$$\liminf_{\delta\to 0} \mathcal{E}_\delta(v_\delta, v_\delta) \geq \mathcal{E}(v, v).$$

For a finite lower limit, apply the extractions on a countable exhaustion to a subsequence realizing that limit.

Equation (50) proves, in particular, that the radial coefficient is exactly θ. The original metric in (41) has no radial–angular product, and its minimizing periodic adjustment only changes the angular derivative. Consequently the limiting energy has no mixed radial–angular term.

6. Approximating the energy from above. We first treat a smooth v on $\overline{B}_R$. Put $w = v \circ X$ on each face. For every (r, y) choose the normalized minimizing cell function

$$\zeta_*(r, y, z) = \zeta(G(y)^{-1}, \nabla_y w(r, y)).$$

It depends continuously on (r, y) with values in $H^1(Y_h)$, by the estimate following (47), and is bounded there for this fixed h. Extend it into the full periodic square by the fixed-cell extension described above.

Cutting off in (r, y) and then convolving, periodically in z, approximates these extensions in $L^2((1, R) \times Q; H^1_{\text{per}}(Y))$ by smooth functions $W(r, y, z)$, periodic in z, whose support in (r, y) is compactly contained in $(1, R) \times Q$. Dominated convergence justifies the cutoffs; derivatives in (r, y) are not part of this norm. Since the quadratic integrals are continuous in $\nabla_z W$ for this norm,

$$\sum_{\text{faces}} \int_1^R \int_Q J(y) \int_{Y_h} (\nabla_y w + \nabla_z W)^{\mathsf{T}} G^{-1} (\nabla_y w + \nabla_z W)\, dz\, dy\, dr \tag{53}$$

can be made arbitrarily close to the limiting angular energy. Thus the exclusions near $r = 1$ and the face boundaries have arbitrarily small energy cost before δ is sent to zero.

Keep such smooth functions W fixed for the moment. Define a function on the full ball by

$$V_\delta(x) = v(x) \quad (|x| \leq 1), \qquad V_\delta(X(r, y)) = w(r, y) + \delta W(r, y, y/\delta) \quad (1 < r < R). \tag{54}$$

The second definition is made separately on each open face. Because W vanishes near all face boundaries and near $r = 1$, the definitions agree on their overlaps and traces. Thus $V_\delta \in H^1(B_R)$, and $V_\delta \to v$ in $L^2(B_R)$. Set $v_\delta = V_\delta|_{\Omega_\delta}$. Differentiation gives

$$\partial_r(V_\delta \circ X) = \partial_r w + \delta \partial_r W(r, y, y/\delta),$$

and

$$\nabla_y(V_\delta \circ X) = \nabla_y w + \nabla_z W(r, y, y/\delta) + \delta \nabla_y W(r, y, y/\delta).$$

The terms multiplied by δ tend uniformly to zero for these fixed smooth W. Periodic averaging on complete period squares and (41) now prove convergence of the radial energy to $\theta \int r^2|\partial_r v|^2\, dr\, dS$,

and convergence of the angular energy to (53). The additionally retained coordinate strips have area $O(\delta)$; since W is zero near them, their energy is at most $C\delta$. The energy in the unit ball is exactly that of v.

Choose successive W_n with angular energy error at most $1/n$, and then thresholds $d_n \downarrow 0$ below which the fixed-W_n convergence errors are at most $1/n$. Using W_n when $d_{n+1} \le \delta < d_n$ gives

$$\mathcal{E}_\delta(v_\delta, v_\delta) \longrightarrow \mathcal{E}(v, v), \qquad \|v_\delta - v\|_{L^2(\Omega_\delta)} \longrightarrow 0. \tag{55}$$

The extensions $E_\delta v_\delta$ are bounded in H^1. For any strong L^2 subsequential limit a, (48) applied to $E_\delta v_\delta - v$ gives

$$\int_{B_R} m|a - v|^2\, dx = \lim \int_{\Omega_\delta} |v_\delta - v|^2\, dx = 0.$$

Since $m \ge \theta > 0$, every such limit equals v, proving convergence of the full extended sequence. Smooth density in $H^1(B_R)$, continuity of the limiting norm and energy, and a second diagonal choice give the recovery sequence for general $v \in H^1(B_R)$.

7. Indexed eigenvalues. For fixed R, h, the limiting norm and energy are equivalent to the usual L^2 norm and gradient energy, by (15). Compact embedding therefore gives a discrete spectrum and the min–max formula.

Take individual recovery sequences for the first $k+1$ limiting orthonormal eigenfunctions $e_0, \dots, e_k$. Their mass matrices converge to the identity. Their energy matrices are bounded by Cauchy–Schwarz, and any subsequential limit M satisfies, by the lower bound,

$$a^\mathsf{T} M a \ge \mathcal{E}\Big(\sum_i a_i e_i, \sum_i a_i e_i\Big) \quad (a \in \mathbb{R}^{k+1}).$$

The difference of these quadratic forms is positive semidefinite with zero diagonal, since each individual sequence recovers its energy, and hence is zero. Thus the energy matrices converge, without requiring linear recovery choices. The min–max formula on their spans gives

$$\limsup_{\delta \to 0} \lambda_k(\Omega_\delta) \le \lambda_k.$$

Conversely, along a subsequence realizing $\ell = \liminf \lambda_k(\Omega_\delta)$, extract simultaneous limits of the extensions of the first $k+1$ orthonormal actual eigenfunctions $u_{0,\delta}, \dots, u_{k,\delta}$. The upper bound bounds their energies, and (48) makes the limits $u_0, \dots, u_k$ weighted orthonormal. Since

$$\mathcal{E}_\delta\Big(\sum_i a_i u_{i,\delta}, \sum_i a_i u_{i,\delta}\Big) \le \lambda_k(\Omega_\delta) \sum_i a_i^2,$$

the lower energy bound and limiting min–max formula give $\lambda_k \le \ell$. This proves indexed convergence with multiplicities.

8. The first eigenfunction and simplicity. Suppose λ_1 is simple. Then $\lambda_1 < \lambda_2$, so indexed convergence implies $\lambda_1(\Omega_\delta) < \lambda_2(\Omega_\delta)$ for all sufficiently small δ. Thus the actual first positive eigenvalue is simple. Every strong L^2 limit of its normalized extended eigenfunctions has weighted norm one, weighted mean zero, and, by the lower bound, energy at most λ_1. It is therefore a

minimizer for the first positive limiting eigenvalue. Simplicity makes it equal to u_0 or $-u_0$, where u_0 is any fixed normalized real limiting eigenfunction. Choose the sign so that

$$\int_{\Omega_\delta} u_\delta u_0 \, dx > 0.$$

This integral tends along each convergent subsequence to $\langle u, u_0 \rangle_m = \pm 1$, so it is nonzero for all sufficiently small δ and the chosen limit is always u_0. Compactness then proves convergence of the entire signed sequence. This completes every assertion of Lemma 3. □

6.4 Proof of Lemma 4

Fix R, θ. The extension lemma and the Sobolev inequality on the fixed ball give, uniformly in δ,

$$\|z\|^2_{L^6(\Omega_\delta)} \le S\Big(\|\nabla z\|^2_{L^2(\Omega_\delta)} + \|z\|^2_{L^2(\Omega_\delta)}\Big), \qquad z \in H^1(\Omega_\delta). \tag{56}$$

All constants in the boundedness estimates below depend only on S and, for the global estimate, the eigenvalue bound Λ.

Put $D_t = \Omega_\delta \cap B(x,t)$. The local weak formulation is

$$\int_{D_{2s}} \nabla v \cdot \nabla \varphi \, dx = \int_{D_{2s}} F \varphi \, dx \tag{57}$$

for every $\varphi \in H^1(D_{2s})$ whose support stays a positive distance from $\partial B(x, 2s)$. The test function may be nonzero on $\partial \Omega_\delta$.

The local estimate. Take $s_0 \le 1$, write $f = \|F\|_{L^\infty(D_{2s})}$, and set $a = s^2 f + \varepsilon$, $w = (v-c)_+ + a$, where $\varepsilon > 0$. Testing (57) with an increasing approximation to the indicator of $\{v > c\}$ times a nonnegative test function gives $\int \nabla w \cdot \nabla \psi \le f \int \psi$. For $p \ge 2$ and a Lipschitz cutoff η supported strictly inside $B(x, 2s)$, testing this inequality with $\eta^2 w^{p-1}$ and using Young's inequality gives

$$\int_{D_{2s}} |\nabla(\eta w^{p/2})|^2 \le C p^2 \int_{D_{2s}} w^p (|\nabla \eta|^2 + s^{-2}\eta^2),$$

since $f/w \le f/a \le s^{-2}$. These tests do not assume boundedness: use $\eta^2 w \min(w, L)^{p-2}$ first and pass to the limit as $L \to \infty$. The estimate is then valid whenever $w \in L^p$.

Extend $\eta w^{p/2}$ by zero to the rest of Ω_δ and apply (56). Choosing $\eta = 1$ on $B(x, t')$, supported in $B(x,t)$, with $|\nabla \eta| \le C/(t-t')$, yields

$$\|w\|_{L^{3p}(D_{t'})} \le \big[CSp^2((t-t')^{-2} + s^{-2})\big]^{1/p} \|w\|_{L^p(D_t)}, \qquad s \le t' < t \le 2s.$$

The endpoint $t = 2s$ follows by approximation with cutoffs supported strictly inside that ball. Iterate with $p_j = 2 \cdot 3^j$ and $t_j = s(1 + 2^{-j})$. Since $\sum_j p_j^{-1} = 3/4$ and $\sum_j j/p_j < \infty$, this gives

$$\|w\|_{L^\infty(D_s)} \le C s^{-3/2} \|w\|_{L^2(D_{2s})} \le C\big(s^{-3/2}\|v-c\|_{L^2(D_{2s})} + a\big),$$

where the last inequality uses $|D_{2s}| \le C s^3$. Let $\varepsilon \downarrow 0$ and repeat for $(c-v)_+$ to obtain (21). Only (56) and Euclidean cutoffs were used, so the constants remain uniform near every boundary piece and its corners.

The global bound and boundary values. For a normalized Neumann eigenfunction with $0 \le \lambda \le \Lambda$, testing the equation with $|u|^{p-2}u$, justified by truncation as above, and applying (56) gives

$$\|u\|_{L^{3p}(\Omega_\delta)} \le \left[CSp^2(1+\Lambda)\right]^{1/p}\|u\|_{L^p(\Omega_\delta)}, \qquad p \ge 2.$$

Iteration starting at $p = 2$ proves (22), with a constant depending only on R, θ, Λ. In particular, λu is bounded. For each fixed δ, the domain is bounded and Lipschitz, so the Neumann boundary regularity theorem [17, Proposition 3.6] gives a continuous representative of u on $\overline{\Omega}_\delta$. No uniform boundary modulus of continuity is needed. By continuity, the essential-supremum bound (21) also holds at boundary points, which are limits of interior points. □

6.5 Proof of Lemma 5

In this proof only the constant weight θ used for the basic starlike construction is considered. Write

$$d\mu(r) = 4\pi p(r)\,dr, \qquad p(r) = \begin{cases} r^2, & 0 < r < 1, \\ \theta r^2, & 1 < r < R. \end{cases}$$

The Rayleigh quotient on the radial subspace is

$$\frac{\int_0^R p(r)|v'(r)|^2\,dr}{\int_0^R p(r)|v(r)|^2\,dr}, \qquad \int_0^R p(r)v(r)\,dr = 0.$$

The factors 4π cancel. Define the continuous test function

$$g(r) = \begin{cases} 1, & 0 \le r \le 1, \\ \dfrac{1/r - 1/R}{1 - 1/R}, & 1 \le r \le R. \end{cases}$$

Its radial extension belongs to $H^1(B_R)$. Its derivative has a jump only at $r = 1$, where g itself is continuous. Direct integration gives

$$\int_0^R p(r)\,dr = \frac{1+\theta(R^3-1)}{3},$$
$$\int_0^R p(r)g(r)\,dr = \frac{1}{3} + \frac{\theta(R-1)(R+2)}{6},$$
$$\int_0^R p(r)|g'(r)|^2\,dr = \frac{\theta}{1-1/R}.$$

Let

$$b_R = \frac{\int_0^R pg}{\int_0^R p} = \frac{1+\theta(R-1)(R+2)/2}{1+\theta(R^3-1)}.$$

For $\theta = R^{-5/2}/(4\pi)$, the numerator tends to 1, whereas the denominator is asymptotic to $R^{1/2}/(4\pi)$. Thus $b_R \to 0$. For all sufficiently large R, we have $0 < b_R \le 1/2$.

The function $g - b_R$ has the required mean zero. On $[0,1]$ it equals $1 - b_R$, so

$$\int_0^R p(r)(g(r)-b_R)^2\,dr \ge \frac{(1-b_R)^2}{3} \ge \frac{1}{12}.$$

Its energy is unchanged by subtracting the constant. For $R \geq 2$, the variational characterization therefore yields

$$\lambda_{\text{rad}} \leq \frac{\theta/(1-1/R)}{1/12} \leq 24\theta = \frac{6}{\pi} R^{-5/2}.$$

This proves (23) with a constant independent of R. □

6.6 Proof of Lemma 6

We first justify the variational eigenfunction and its boundary conditions, including the condition at the singular endpoint 0. For the fixed R and $\theta > 0$ under consideration, the weighted norm is equivalent to the ordinary $L^2(B_R)$ norm, and the weighted energy is equivalent to the ordinary Dirichlet energy. The radial subspace of $H^1(B_R)$ is closed. The compact embedding $H^1(B_R) \to L^2(B_R)$ and the Poincaré inequality on the ball therefore give a minimizer f for

$$\lambda_{\text{rad}} = \inf \left\{ \frac{\int_0^R p(v')^2}{\int_0^R pv^2} : v(|\cdot|) \in H^1(B_R), \quad v \neq 0, \quad \int_0^R pv = 0 \right\}.$$

In particular $\lambda_{\text{rad}} > 0$. A minimizing sequence may be normalized by $\int_0^R pv^2 = 1$. Its energies and its ordinary H^1 norms are bounded; its weak H^1 limit is radial, and strong L^2 convergence preserves both the normalization and the mean condition. Lower semicontinuity of the energy then gives the stated minimizer.

Put $\lambda = \lambda_{\text{rad}}$. Differentiating the Rayleigh quotient along mean-zero radial variations gives

$$\int_0^R pf'\varphi' \, dr = \lambda \int_0^R pf\varphi \, dr \tag{58}$$

for every mean-zero radial test function. Subtracting a constant from an arbitrary radial test function does not change its derivative; it also does not change the right side, since $\int_0^R pf = 0$. Consequently (58) holds for every radial test function.

On each of $(0,1)$ and $(1,R)$, distributional differentiation gives

$$-(pf')' = \lambda pf. \tag{59}$$

On compact subintervals away from 0, both p and p^{-1} are bounded. The equation implies that pf' is absolutely continuous there. Since p is smooth on each of the two intervals, the solution is smooth there. The function f is continuous at 1, because a one-dimensional H^1 function on a neighborhood of 1 is continuous. Integrating (58) by parts on the two intervals, using test functions supported near 1, gives

$$p(1-)f'(1-) = p(1+)f'(1+).$$

Using tests supported near R, with an arbitrary value at R, gives $p(R)f'(R) = 0$, hence $f'(R) = 0$.

The endpoint 0. Let $k = \sqrt{\lambda}$. In $(0,1)$ equation (59) is $f'' + 2f'/r + \lambda f = 0$. Substituting $w(r) = rf(r)$ gives $w'' + \lambda w = 0$. Hence

$$f(r) = \frac{a\sin(kr) + b\cos(kr)}{r}, \qquad 0 < r < 1.$$

If $b \neq 0$, then $f'(r) = -b/r^2 + O(1)$ as $r \downarrow 0$, which would give $\int_0^1 r^2 |f'(r)|^2 \, dr = \infty$. The finite-energy condition therefore forces $b = 0$. The remaining solution extends smoothly across 0 as a radial function and has

$$f(0) = ak, \qquad f'(0) = 0, \qquad f(r) = f(0)\frac{\sin(kr)}{kr}, \qquad \lim_{r \downarrow 0} p(r) f'(r) = 0. \tag{60}$$

The coefficient a is nonzero: otherwise f vanishes in the unit ball, and the value and flux at 1 vanish. Uniqueness for the ordinary differential equation on $[1, R]$ would then make f identically zero, a contradiction. Thus $f(0) \neq 0$, and its sign can be chosen positive.

Simplicity. Any radial eigenfunction with eigenvalue $\lambda > 0$ satisfies the same finite-energy condition at 0. By (60), it is uniquely determined on $[0, 1]$ by its value at 0. Continuity and flux continuity specify its value and derivative at $1+$, and uniqueness for the differential equation then specifies it on $[1, R]$. Two radial eigenfunctions with eigenvalue λ are therefore proportional. In particular the first positive radial eigenvalue is simple.

The number of zeros. There is at least one zero in $(0, R)$, since f is nonzero and $\int_0^R pf = 0$. A zero in either smooth interval is simple: if both f and pf' vanished there, uniqueness for the equation would imply $f \equiv 0$. The same argument works at 1, using flux continuity. Also $f(R) \neq 0$, since otherwise the Neumann condition would give both value and derivative zero at R. Formula (60) excludes zeros close to 0. Zeros cannot accumulate in the remainder of $[0, R]$, because an accumulation point would have both value and derivative (or value and flux, at 1) zero. Thus there are finitely many zeros, and the intervals between consecutive zeros are precisely the intervals on which f has a fixed nonzero sign.

Suppose there were at least three such intervals. Choose two of them, I_1 and I_2, and let f_j be f on I_j and zero elsewhere. Their radial extensions belong to $H^1(B_R)$: at each internal endpoint $f = 0$, so the zero extension introduces no jump. Testing (58) with f_j gives

$$\int_0^R p(f_j')^2 \, dr = \lambda \int_0^R p f_j^2 \, dr.$$

Each number $m_j = \int_0^R p f_j \, dr$ is nonzero, because f_j has a fixed nonzero sign on its interval. Set

$$v = m_2 f_1 - m_1 f_2.$$

This is a nonzero radial function with $\int_0^R pv = 0$. Since f_1 and f_2 have disjoint interiors of support, their mass and energy cross terms vanish. Therefore

$$\int_0^R p(v')^2 \, dr = \lambda \int_0^R p v^2 \, dr.$$

Thus v is another minimizer for the first positive radial Rayleigh quotient, and the variational argument above shows that it is a radial eigenfunction with eigenvalue λ. Simplicity makes v proportional to f. But v vanishes on the third sign interval, where f does not vanish. This is impossible. There are therefore exactly two sign intervals, separated by exactly one zero $z \in (0, R)$.

Strict decrease. The chosen sign gives $f > 0$ on $[0, z)$ and $f < 0$ on $(z, R]$. Define $J(r) = \int_0^r p(s) f(s) \, ds$. Then $J(r) > 0$ for $0 < r \leq z$. If $z < r < R$, the mean-zero condition gives

$$J(r) = -\int_r^R p(s) f(s) \, ds > 0.$$

Integrating (59), using (60) and the flux condition at 1, gives

$$p(r)f'(r) = -\lambda J(r) < 0 \qquad (0 < r < R),$$

with the derivative interpreted one-sidedly at 1. The function is therefore strictly decreasing on $[0, R]$. This proves every assertion of Lemma 6, and also proves the monotonicity used in the main argument. □

References

[1] R. Atar and K. Burdzy. On Neumann eigenfunctions in lip domains. *J. Amer. Math. Soc.* **17** (2004), 243–265.

[2] R. Bañuelos and K. Burdzy. On the "hot spots" conjecture of J. Rauch. *J. Funct. Anal.* **164** (1999), 1–33.

[3] R. F. Bass and K. Burdzy. Fiber Brownian motion and the "hot spots" problem. *Duke Math. J.* **105** (2000), 25–58.

[4] K. Burdzy. The hot spots problem in planar domains with one hole. *Duke Math. J.* **129** (2005), 481–502.

[5] K. Burdzy. Overview of the "hot spots" problem. In *Brownian Motion and its Applications to Mathematical Analysis*, Lecture Notes in Mathematics, vol. 2106, Springer, 2014, pp. 21–29.

[6] K. Burdzy. Removing boundary smoothness from the hot-spots conclusion in the simple-eigenvalue case. Preprint, 2026. arXiv:2610.12622.

[7] K. Burdzy and W. Werner. A counterexample to the "hot spots" conjecture. *Ann. of Math.* (2) **149** (1999), 309–317. arXiv:math/9803030.

[8] D. Cioranescu, A. Damlamian and G. Griso. Periodic unfolding and homogenization. *C. R. Math. Acad. Sci. Paris* **335** (2002), 99–104.

[9] J. de Dios Pont. Convex sets can have interior hot spots. Preprint, 2024. arXiv:2412.06344.

[10] J. de Dios Pont, A. W. Hsu and M. A. Taylor. Sharp bounds on the failure of the hot spots conjecture. Preprint, 2025. arXiv:2508.16321.

[11] L. C. Evans. *Partial Differential Equations*, second edition. Graduate Studies in Mathematics, vol. 19, American Mathematical Society, 2010.

[12] D. Jerison and N. Nadirashvili. The "hot spots" conjecture for domains with two axes of symmetry. *J. Amer. Math. Soc.* **13** (2000), 741–772.

[13] C. Judge and S. Mondal. Euclidean triangles have no hot spots. *Ann. of Math.* (2) **191** (2020), 167–211.

[14] C. Judge and S. Mondal. Erratum: Euclidean triangles have no hot spots. *Ann. of Math.* (2) **195** (2022), 337–362.

[15] J. B. Kennedy and J. Rohleder. On the hot spots conjecture in higher dimensions. *Trans. Amer. Math. Soc. Ser. B* **13** (2026), 108–131.

[16] A. Kleefeld. The hot spots conjecture can be false: some numerical examples. *Adv. Comput. Math.* **47** (2021), article 85.

[17] R. Nittka. Regularity of solutions of linear second order elliptic and parabolic boundary value problems on Lipschitz domains. *J. Differential Equations* **251** (2011), 860–880.

[18] OpenAI. Strict hot spots and absence of interior critical points on smooth simply connected planar domains. Manuscript, September 24, 2026. Manuscript available online.

[19] M. N. Pascu. Scaling coupling of reflecting Brownian motions and the hot spots problem. *Trans. Amer. Math. Soc.* **354** (2002), 4681–4702.

[20] J. Rauch. Five problems: an introduction to the qualitative theory of partial differential equations. In *Partial Differential Equations and Related Topics*, J. A. Goldstein (ed.), Lecture Notes in Mathematics, vol. 446, Springer, 1975, pp. 355–369.

[21] J. Weber. *Introduction to Sobolev Spaces*. Lecture notes, revised November 17, 2025. https://www.math.stonybrook.edu/~joa/PUBLICATIONS/SOBOLEV.pdf.